FEATURE ARTICLE

Structure–property relationships of iron arsenide superconductors

Dirk Johrendt*

Iron based superconductors sent material scientists into a renewed excitement reminiscent of the time when the first high-T_c superconductors were discovered 25 years ago. This feature article reviews relationships between structural chemistry and magnetic as well as superconducting properties of iron arsenide compounds, which are outstandingly rich and uniquely coupled. Particular attention is paid to the nature of the structural phase transitions of the parent compounds and their possible origins, on effects of doping on the crystal structures and on the coexistence of magnetic ordering and superconductivity. In spite of the many fascinating insights that have already enriched the research on superconductivity, many questions are still open and prove iron based superconductors to be a good recipe for future discoveries in this lively field.

Introduction

Superconductivity persistently survives among the biggest challenges of solid-state chemistry and physics. Even a century after the discovery of the phenomenon, scientists still do not completely understand how pairs of conduction electrons glue together and flow through solids without any resistivity at temperatures as high as 140 K. Meanwhile, the large number and

Department Chemie, Ludwig-Maximilians-Universität, München, Germany. E-mail: dirk.johrendt@cup.uni-muenchen.de; Fax: +49 (0)89 2180 77431; Tel: +49 (0)89 2180 77430

Dirk Johrendt

Dirk Johrendt was born in Oberhausen, Germany, and received his PhD in chemistry in 1993 from the University of Cologne under the supervision of Prof. Albrecht Mewis with a thesis on transition metal pnictides. He was a postdoctoral fellow with Prof. Jean Rouxel at the IMN Nantes, France, where he worked on misfit layer compounds. He completed his habilitation in 2001 at the University of Düsseldorf and became a professor of inorganic solid state chemistry at the Ludwig-Maximilians-Univer-sity München in 2002. Research interests of his group are synthesis, crystal structures and physical property relations of highly correlated, magnetic and superconducting inorganic solid state materials.

great variety of superconducting compounds may be indicative of a universal property of matter, which can appear in almost any class of material with mobile electrons at sufficiently low temperatures. Indeed, all search strategies or recipes for superconductors have proved to be incorrect[1] and new superconductors repeatedly have been discovered in fields never expected before. Moreover, alleged rules could have even hampered the progress. The recent discovery of high-temperature superconductivity in iron compounds constitutes a hortative example for such a baseless prejudice. These iron compounds were known for decades, but were not seriously considered as potential superconductors, arguably because iron metal is the archetypal ferromagnet, and ferromagnetism destroys superconductivity. Even though the latter is true, it is of course obstructive and simply wrong to generalize all iron compounds, which are self-evidently not inherently ferromagnetic. This again teaches us the lesson not to exclude any material due to properties of its components. However, the liberation of iron required fortuity, which appeared with the discovery of superconductivity in LaFePO,[2] LaFeAsO,[3] and related compounds with critical temperatures up to 55 K.[4]

This has opened a new chapter in superconductor research, and was arguably the most important breakthrough in this field for more than two decades. The discovery sent physicists and materials scientists into a renewed excitement reminiscent of the time of the first high-temperature superconductors more than 20 years ago. Besides the fascinating richness of structural and physical properties and despite many still open issues, these materials provide new avenues for understanding the phenomenon and may finally foster more reliable rules.[5] Only three years after the discovery, enormous progress has already been made. This may be partially owing to methods, instrumentation and experiences, that had been developed over decades of studying cuprates. More than 2000 papers are already published and the

current state of knowledge is repeatedly summarized in excellent review articles.[6]

Even though the mystery of the physical mechanism of superconductivity at higher temperatures is still not resolved, some pieces could be added to the puzzle. Actually, it sounds like an irony of fate that iron based superconductors provide just magnetism as an important ingredient to induce high-T_c super-conductivity. However, the formation of Cooper pairs by magnetic spin fluctuations (spin-density-waves) is no new idea. It was discussed for cuprate superconductors years ago[7] and is highly controversial to this day. But the iron compounds apparently provide a new flavour of this approach. Instead of the anisotropic (d-wave)[8] symmetry of the superconducting gap in cuprates, iron based superconductors get along with an isotropic, sign-reversing gap ($s^{\pm}$-wave).[9] This has crucial implications not only to theory. Indeed, the anisotropic superconducting properties are the big drawback of cuprate superconductors in terms of technical applicability. Iron based superconductors do not suffer from such anisotropies, and even though their critical temperatures are still lower, the development of films[10,11] or wires[12] with these new materials is going ahead.

Magnetism is not only presumed to play an important role in the pairing mechanism. Additionally, magnetic properties of iron based superconductors are exceptionally strong coupled to structural degrees of freedom. In other words, the role of the lattice, or more specifically, the details of the crystal structures, carry greater weight in iron arsenides than in cuprates. Obvious manifestations of lattice effects are still unclear isotope effects[13–15] and the widely studied magneto-structural phase transitions that have been observed in most, but not all, iron based superconductors. Only after these transitions are suppressed by doping or pressure does superconductivity emerge with the highest critical temperatures and fields. Other seemingly small details of the crystal structures, among them tiny changes of the composition, variations of bond lengths and/or angles, as well as different responses of the structure to doping, have been found to affect the magnetic state and thereby superconductivity. Finally, a unique coupling of superconductivity, antiferromagnetic ordering and structural changes was observed in iron arsenide materials.

This outstanding interplay between magnetism, super-conductivity and the crystal structure makes iron based super-conductors especially interesting in solid state and structural chemistry. In this feature article, structural effects occurring in the different type of materials are reviewed within the framework of the current state of knowledge about this new class of super-conducting compounds.

Materials and basic structures

The basic crystal structures of the iron based superconductors are shown in Fig. 1. They belong to well known structure families, and most of them have been studied for decades. Iron sele-nide β-FeSe with the tetragonal $anti$-PbO-type structure[16] may be considered as the archetypal material. Edge-sharing $FeSe_{4/4}$-tetrahedra form quasi two-dimensional layers perpendicular to the c-axis of the tetragonal space group $P4/nmm$. Even more general, this structure can be derived from a cubic closest packing (ccp) of selenium atoms, where every second layer of tetrahedral holes is filled by iron atoms. By additional filling of the
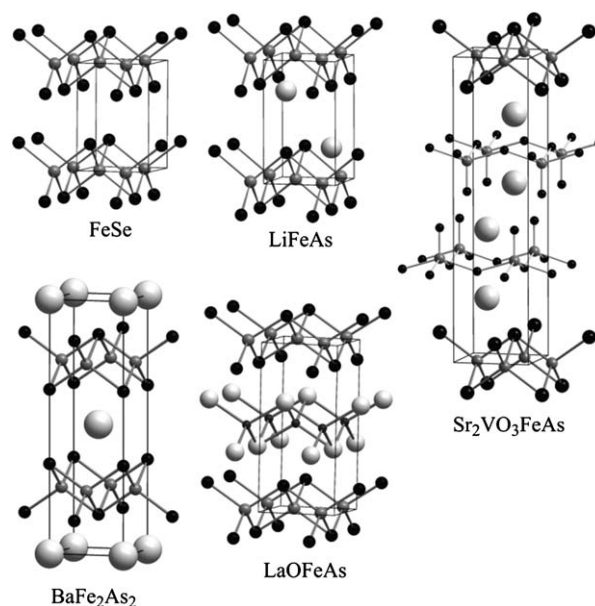

Fig. 1 Crystal structures of iron based superconductors: FeSe, LiFeAs, LaOFeAs and Sr_2VO_3FeAs crystallize in space group $P4/nmm$, $BaFe_2As_2$ in $I4/mmm$. Iron atoms are represented by dark grey spheres, arsenic (selenium) by black spheres. Light grey balls are larger cations between the layers. All structures are tetragonal with the c-axis pointing up.

octahedral holes and shifting their positions along an elongated c-axis, we generate the tetragonal $anti$-PbFCl-type, which is the structure of the '111'-superconductors LiFeAs[17] and NaFeAs.[18] If we add additional atoms into the second layer of tetrahedal holes, we arrive at the ZrCuSiAs-type,[19] which is a filled variant of the PbFCl-type structure, and adopted by the '1111' super-conductors like LaOFeAs.[20] Also the $ThCr_2Si_2$-type structure of the 122-superconductors like $BaFe_2As_2$[21] and the newly discov-ered selenides $K_xFe_{2-y}Se_2$[22] can be derived from closest packing. Imagine a c-axis elongated ccp of barium atoms, where iron occupies all tetrahedral holes and all octahedral holes are filled by As–As dumbbells. Finally, also the structures of the more complicated compounds like Sr_2VO_3FeAs[23] (Fig. 1, right) which crystallizes in the Sr_2GaO_3CuS-type structure,[24] can be consid-ered as derivatives of a strongly distorted ccp-motif.

Phase transitions of the parent compounds

LaOFeAs

Stoichiometric LaOFeAs is not superconducting, but a poor metal. The specific resistivity (ρ) is some orders of magnitude larger than that of good metals like copper or aluminium. An anomaly in $\rho(T)$ at about 150 K was already recognized in the pioneering paper by Kamihara et al.,[3] but the reason for the drop of the resistivity shown in Fig. 2 (black curve) was unclear at that time.

Early DFT electronic band structure calculations of LaOFeP[26] and LaOFeAs[27,28] revealed both materials as magnetic semi-metals with significantly two-dimensional character of the Fermi-surfaces. A semimetal is a true metal with a special feature in the band structure as sketched in Fig. 3. It may be considered as a semiconductor where the filled valence band and the empty
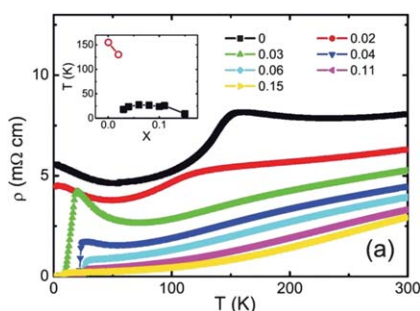
Fig. 2 Resistivity of La(O$_{1-x}$F$_x$)FeAs showing the gradual suppression of the anomaly at 150 K in stoichiometric LaOFeAs (black curve) by F-doping. Superconductivity emerges at $x \approx 0.03$ (nominal), where the effect is no longer visible. Figure from ref. 25.

Fig. 4 (a) Fermi surface section of LaOFeAs at $k_z = 0$. Blue circles represent the cylinders around the M- (electron-like) and Γ-points (hole-like). Red: cylinder around M shifted by the nesting vector $q = (\pi, \pi, 0)$. (b) Lindhard response function $\chi_0(q)$, which is strongly peaked at the nesting vector. Figures from ref. 25.

conduction band are shifted in energy and slightly overlap. Electrons are virtually decanted from the filled band into the empty one, forming so-called hole-pockets and electron pockets. States at the Fermi-level are denoted as hole-like and electron-like, respectively.

It turned out that LaOFeAs has an additional feature: Cylinder-shaped sheets of the Fermi-surface, originating from the hole-like and electron-like bands, have very similar radii and coincide when shifted by a certain reciprocal space vector **q**. Theoretical evidence of this Fermi-surface nesting in LaOFeAs was first shown by Dong *et al.*,[25] who presented the $k_z = 0$ section of the Fermi surface imaged in Fig. 4a. The electron-like sheet around M can be shifted by the nesting vector $q = (\pi, \pi, 0)$ and coincides almost exactly with the hole-like cylinder around Γ. The nesting causes a significant peak in the calculated static susceptibility $\chi_0(q)$, indicating an electronic and/or magnetic instability (Fig. 4b). From these findings the authors proposed either charge-density-wave (CDW) or spin-density-wave (SDW) ordering and suggested a stripe-type magnetic ordering pattern. They also considered the possible formation of spin nematic order that breaks the 4-fold symmetry of the lattice,[29] a concept that has been revisited very recently.[30] Increasing F-doping of La(O$_{1-x}$F$_x$)FeAs slightly changes the topology of the Fermi surface and diminishes the sensitive nesting, until the resistivity anomaly vanishes and superconductivity emerges at $x \approx 0.03$ (see Fig. 2).

The proposed antiferromagnetic ordering of stoichiometric LaOFeAs was immediately verified experimentally *via* neutron diffraction by de la Cruz *et al.*[31] Additionally, a structural distortion was detected at $T_S \approx 155$ K, a temperature significantly above the Néel point $T_N \approx 137$ K. The low-temperature structure was first described in the monoclinic space group
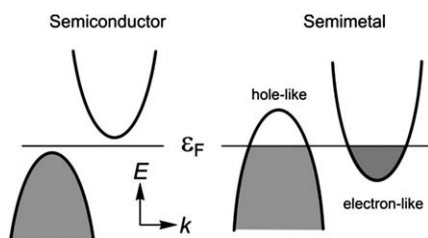

Fig. 3 Sketch of the electronic structure of a semimetal in one-dimensional k-space as developing from a semiconductor. Shaded areas represent filled electron states.
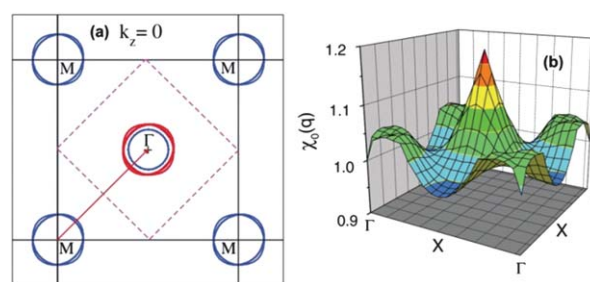
$P112/n$ ($a = 4.0275(2)$, $b = 4.0275(2)$, $c = 8.7262(5)$ Å, $\gamma = 90.279$ (3)°). The authors already mentioned that orthorhombic symmetry may also be possible if the z-coordinates of iron and oxygen would be exactly $\frac{1}{2}$ and 0, respectively, to comply with the special positions $2a$ and $2c$. Actually, the refined coordinates were $z_{Fe} = 0.5006(12)$ and $z_O = -0.0057(17)$ which are equal to $\frac{1}{2}$ and 0 within the experimental error. However, the correct orthorhombic space group $Cmme$ ($a = 5.68262(3)$, $b = 5.71043$ (3), $c = 8.71964(4)$ Å, $T = 120$ K) was given almost at the same time by Nomura *et al.*[32] from X-ray synchrotron data.

Orthorhombic symmetry is also more plausible in terms of a group-subgroup consideration, because $Cmme$ is a maximal subgroup of $P4/nmm$, but $P112/n$ is not. Thus, the observed structural distortion is a translation equivalent (*translationengleiche*) transition of index 2. The unit cell transformation of the tetragonal lattice parameters ($a_o = \frac{1}{2}(a_t - b_t)$, $b_o = \frac{1}{2}(a_t + b_t)$, $c_o = c_t$) is exactly as expected from the nesting vector $(\pi, \pi, 0)$. It is worth noting that this symmetry reduction leads to a superstructure even though the primitive unit cell is unchanged (no additional reflections appear).

Fig. 5 shows the crystal and magnetic structure of orthorhombic LaOFeAs. The magnetic moments within the ab-plane are antiferromagnetically aligned along the a- and c-axis and ferromagnetically along the b-axis. Note that the antiferromagnetic alignment is always *along the longer* of the orthorhombic a- and b-axis. Even though the crystallographic standard setting would be $a < b$, most authors use a as the longer one.

The magnitude of the ordered magnetic moment was first determined by neutron diffraction to 0.36(5) μ_B per iron atom at 8 K,[31] but recent redeterminations revealed significantly larger values of 0.63(1) μ_B at 2 K,[33] and 0.8 μ_B at 9.5 K.[34]

The structural changes in the course of the phase transition are small (Fig. 5, right). From the view of chemical bonding, only the Fe–Fe distances change considerably by splitting from $4 \times 2.8512(2)$ at 300 K to $2 \times 2.8394(3)$ and $2 \times 2.8531(2)$ at 2 K.[33] The Fe–As bond lengths remain almost constant at 2.408(2) (300 K) and 2.402(2) (2 K), respectively, see Fig. 5. Also the As–Fe–As bond angle hardly changes from 113.85(1)° in the tetragonal phase to 113.67(1)° in the orthorhombic structure. Note that one angle sufficiently determines a tetrahedron with tetragonal symmetry ($\bar{4}2m$). Conveniently, the 2-fold angle ε_2 between iron and arsenic atoms at the same z-coordinate (both As above or below the Fe-layer) should be given, while the
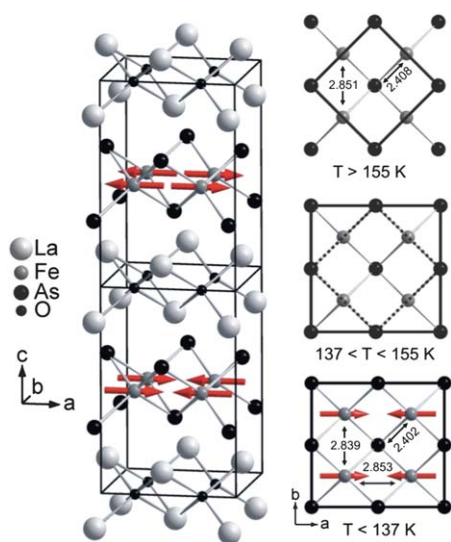
Fig. 5 Left: Crystal and magnetic structure of orthorhombic LaOFeAs. The magnetic unit cell is twice the orthorhombic chemical unit cell. The magnetic moments are antiferromagnetically aligned along the (longer) a-axis and also along c. Right: projections of the FeAs layers at different temperatures. The symmetry is tetragonal ($P4/nmm$) above 155 K and already orthorhombic ($Cmma$) between 155 and 137 K, before long-range magnetic ordering is present below 137 K. Atom distances in Å at 2 K from ref. 33.

4-fold angle ε_4 is simply dependent by the relation cos (ε_4) = $-\frac{1}{2}$ [1 + cos (ε_2)]. Many plots in the literature that give both values are redundant.

As the major contribution to the structural change concerns the lattice parameter a, the degree of distortion is often referred to as orthorhombicity in terms of a structural ordering parameter, defined as $\delta = (a - b)/(a + b)$. Fluoride-doping gradually suppresses the distortion in La$(O_{1-x}F_x)$FeAs as shown in Fig. 6. Whether the phase transitions are completely absent before superconductivity emerges or superconductivity co-exists with magnetic ordering is not completely clear in the 1111-system, where slightly different phase diagrams for $RE(O_{1-x}F_x)$FeAs with RE = La, Ce, Nd, Sm have been published. A detailed discussion of all these phase diagrams is outside the scope of this article; therefore I present only the example of LaO$_{1-x}$F$_x$FeAs in Fig. 7.[35]

In this case, the areas of magnetic order and superconductivity are sharply distinct. This is different in other ZrCuSiAs-type materials, where significant overlaps between the magnetic
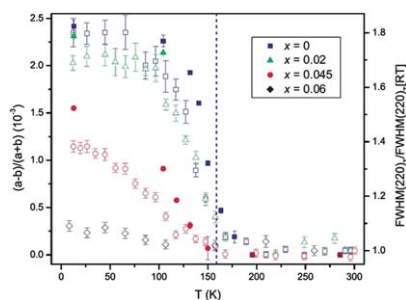

Fig. 6 Temperature dependency of the orthorhombic distortion in La$(O_{1-x}F_x)$FeAs. The sample with $x = 0.06$ (nominal) is not yet super-conducting. Figure from ref. 33

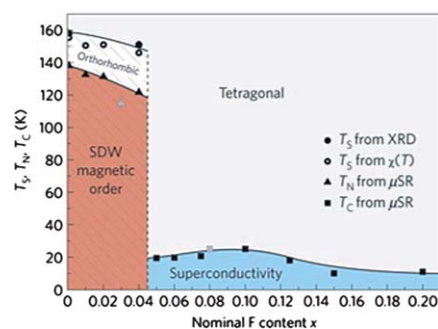**Fig. 7** Phase diagram of LaO$_{1-x}$F$_x$FeAs from ref. 35.

orthorhombic phases and superconductivity were reported. The latter suggests a co-existence of superconductivity with magnetic ordering which has been studied more comprehensibly in doped BaFe$_2$As$_2$. We will come back to this topic later. At this point it is still unclear whether a universal phase diagram of the ZrCuSiAs-type FeAs-superconductors exists.

LiFeAs

In strong contrast to LaOFeAs, the stoichiometric compound LiFeAs[36] is superconducting with T_c up to 18 K[37,38] and shows neither any structural nor magnetic phase transition. Indeed, Borisenko *et al.*[39] reported the absence of Fermi surface nesting from angle-resolved photoemission (ARPES) experiments. On the other hand, DFT calculations[40] revealed a nested Fermi surface topology similar to LaOFeAs, and predicted the same stripe-type antiferromagnetic groundstate.[41] Up to now, no hint to an orthorhombic distortion or magnetic ordering has been detected, in line with the ARPES results. This exceptional behaviour of LiFeAs challenges the often assumed linkage between nesting and superconductivity. But LiFeAs is also a special case from the chemical point of view. The effective ionic radii of Li$^+$ and Fe^{2+} are not very different[42] and lithium is also stable in tetrahedral coordination. Thus certain mixing of Li/Fe at the tetrahedral ($2a$) or octahedral ($2c$) sites of the PbFCl-structure is thinkable. Juza and Langer[17] already considered the lithium-richer composition Li$_{1.1}$FeAs with additional Li atoms at octahedrally coordinated $2b$ positions according to Li^{O1}Li$_{0.1}^{O2}$Fe^{T}As^{ccp} (O1, O2 = octahedral, T = tetrahedral sites) and also iron-richer compositions like (Li$_{0.25}$Fe$_{0.75}$)^{O1}Li$_{0.1}^{O2}$Fe^{T}As^{ccp}. However, recent redeterminations[36,43] by combined synchrotron X-ray and neutron powder diffraction revealed LiFeAs as nearly stoichiometric. Nevertheless, small Li/Fe disorder cannot be ruled out in the end because the scattering power of Li is very small in both X-ray and neutron diffraction. It appears that at least nearly stoichiometric LiFeAs is the superconducting phase, which is also supported by substitution experiments.[43] Small amounts of iron at the lithium site in Li$_{1-y}$Fe$_{1+y}$As as well as doping of the iron site with cobalt or nickel in LiFe$_{1-x}$$M_x$As ($M$ = Co, Ni) rapidly decrease T_c and finally suppress superconductivity.

NaFeAs

The isotypic sodium compound NaFeAs is probably not super-conducting when it is exactly stoichiometric, but to synthesize the

material in the ideal composition turned out to be difficult. Reasons could be the sensitivity to moisture and problems with exactly determining the Na-concentration. Most authors report sodium-deficient $Na_{1-x}FeAs$,[18,44] albeit with scattered results regarding the composition, magnetism, T_c (10–23 K) and superconducting volume fractions. The first study[18] indicated magnetic ordering with a very weak ordered moment of 0.1–0.2 μ_B from μSR data, but initially no additional magnetic scattering in neutron powder patterns. The small ordered moment of 0.09 $\pm$ 0.04 μ_B was later confirmed by single crystal neutron scattering[45] and also a structural transition that occurs near $T_S = 50$ K, well above the Néel temperature of $T_N = 40$ K. The orthorhombicity at 5 K is 1.75×10^{-3}, which is distinctively smaller than in LaOFeAs (2.3×10^{-3}) and in line with the smaller magnetic moment. The single crystals that were used in these experiments were almost stoichiometric $Na_{1-x}FeAs$ with $x \approx 0.01$ according to inductively coupled plasma (ICP) measurements.[46]

Angle resolved photoemission (ARPES) experiments with a NaFeAs single crystal ($T_c = 8$ K, $T_N = 39$ K, $T_S = 54$ K) showed the typically nested hole- and electron pockets.[47] But the authors observed a reconstruction of the electronic structure around T_S and suggested that the structural and magnetic phase transitions may be rather driven by this effect instead of Fermi surface nesting. However, it is accepted that NaFeAs shows structural and magnetic features that are typical for the FeAs parent compounds, but obviously to a much weaker extent. This is also consistent with the results of a study about the effect of Cobalt-doping in $NaFe_{1-x}Co_xAs$.[48] Only 0.1 additional electrons per iron are sufficient to traverse the complete superconducting dome with a maximum T_c of 20 K close to 0.03 excess electrons (Fig. 8). The structural and magnetic transitions are rapidly suppressed by Co-doping and are already absent in $NaFe_{0.975}Co_{0.025}As$.

The reaction of NaFeAs with water and air revealed an unexpectedly interesting topotactic redox chemistry.[49] Water acts as a mild oxidizing agent that removes Na^+ ions from the material by retaining the FeAs-layers. The critical temperature increases up to 25 K. The reaction with oxygen is much faster, removes topotactically up to 50% of the Na-ions and leads to the formation of $NaFe_2As_2$ that has probably the $ThCr_2Si_2$-type structure.[50]

All in all, the properties of NaFeAs are closer to LaFeAsO and $BaFe_2As_2$ than to isostructural LiFeAs in face of the magnetic ground state and the structural transition. However, the latter are very weak and hard to detect; furthermore difficulties in controlling the exact Na-concentration are probably the reasons for scattered results in the literature. Nevertheless, this system
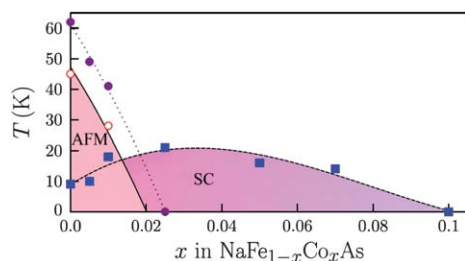
remains very interesting from a chemical point of view with respect to possible exchange reaction of the obviously weakly bonded Na^+ ions between the FeAs layers.

$BaFe_2As_2$

$BaFe_2As_2$ with the tetragonal $ThCr_2Si_2$-type structure[21] contains the same FeAs-layers as LaOFeAs. A certain difference results from the mirror plane perpendicular to the c-axis in the space group $I4/mmm$, which is a glide plane in the space group $P4/nmm$ of LaOFeAs. This mirror plane causes a different stacking of the FeAs-layers in $BaFe_2As_2$, where As-atoms of adjacent layers point to each other, while the layers are mirrored and shifted by $\frac{1}{2}(a + b)$ in LaOFeAs (see Fig. 1).

$BaFe_2As_2$ has early been proposed as a potential parent compound for iron arsenide superconductors[51] with properties very similar to LaOFeAs. The latter was straightforward because of the identical structure and charge of the FeAs-layers in $LaO^+(FeAs)^{1-}$ and $Ba^{2+}[(FeAs)^-]_2$. The structural distortion occurs at 140 K and is also a translation-equivalent (*translationengleiche*) transition of index 2 from the tetragonal space group $I4/mmm$ ($a = 3.9625(1)$, $c = 13.0168(3)$ Å, $Z = 2$) to the orthorhombic space group $Fmmm$ ($a = 5.6146(1)$, $b = 5.5742(1)$, $c = 12.9453(3)$ Å at 20 K). The temperature dependency of the lattice parameters and the typical splitting of the diffraction peaks are depicted in Fig. 9 together with ^{57}Fe-Mössbauer spectra which proved the magnetic ordering. Neutron scattering studies[52–54]
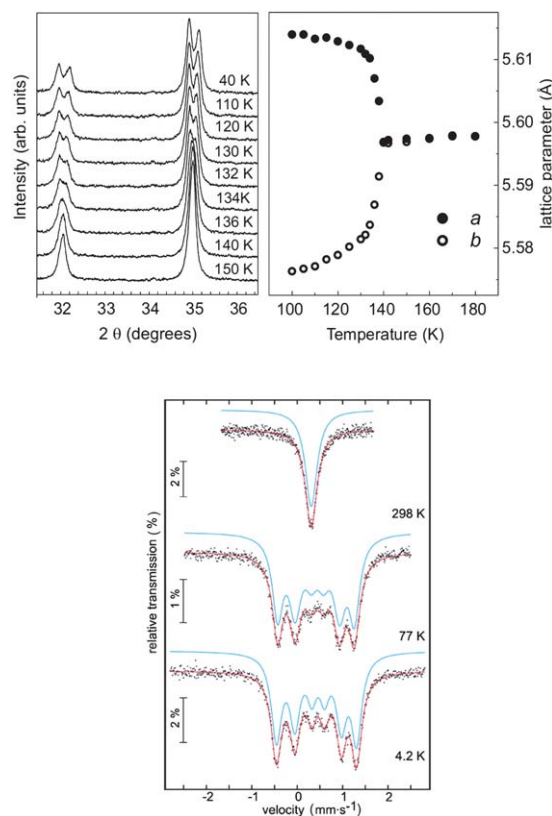

Fig. 9 Top: splitting of diffraction peaks and temperature dependency of the lattice parameters of $BaFe_2As_2$. Bottom: ^{57}Fe-Mössbauer spectra of $BaFe_2As_2$. Figures from ref. 51

Fig. 8 Phase diagram for $NaFe_{1-x}Co_xAs$. Figure from ref. 48

revealed the same stripe-type spin structure as known from LaOFeAs, and it turned out that the Néel-Temperature T_N coincides with T_S where the structural transition occurs, in contrast to LaOFeAs. Due to its continuous character, the structural transition of $BaFe_2As_2$ has been classified as second order in the first report, which caused some debates.[54–56] However, most of the earlier reports contained no detailed studies of the critical behaviour of $BaFe_2As_2$, but have seemingly decided from the 'abruptness' of the transition, especially in the case of iso-structural $SrFe_2As_2$.[57] But recent single crystal neutron diffraction studies[58,59] consistently support the continuous, second order character of the transition, suggesting that some of the scattered results are caused by sample quality. Wilson et al.[60] recently presented an empirical analysis of the magnetic order parameters of $BaFe_2As_2$ and other FeAs-superconductors and showed that both agree well with a 2D-Ising model when $T_N = T_S$. Upon doping, the magnetic and structural order parameters of $BaFe_2As_2$ begin to decouple and behave similarly to LaOFeAs where $T_N < T_S$. The latter can be described with a 3D-Ising model.

A new high-resolution single-crystal X-ray study[61] revealed that the magnetic transition of $BaFe_2As_2$ indeed occurs about 0.75 K *below* the structural one. Fig. 10 shows the orthorhombicity of the crystal close to the transition temperature. An initial second order transition leads from the tetragonal paramagnetic to an orthorhombic paramagnetic phase, which then transforms to the magnetically ordered orthorhombic low temperature phase. These results suggest that $T_N < T_S$ may be universal in iron arsenides.

Even though extensive experimental and theoretical findings were achieved, the underlying origin of the structural and the following magnetic transitions of the iron arsenides are not completely clear. Obviously, the 4-fold rotational symmetry gets broken *before* long range magnetic ordering appears. The reason why the structural and magnetic transition temperatures are separated by ~20 K in LaFeAsO, and even 50 K SrFFeAs[62,63] but occur nearly simultaneously in $BaFe_2As_2$ is not well understood.[51] In a recent X-ray diffraction study, Ricci et al.[64] assign this difference between LaFeAsO and $BaFe_2As_2$ to different elastic constants of the spacer layers. LaO-layers may be more rigid than Ba-layers against the distortion that emanates from the FeAs layers in both cases. Cano et al.[65] have published a theoretical approach based on magneto-elastic coupling which is essentially along this line.
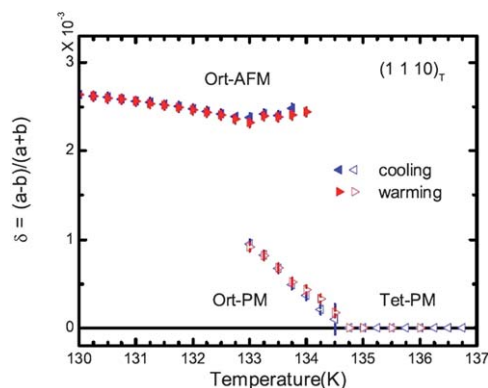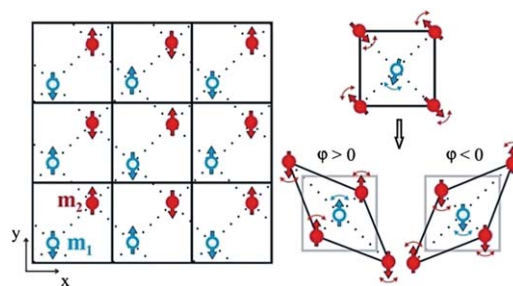

Fig. 11 Left: the two iron atoms form two coupled AFM sublattices magnetization m_1 and m_2. Right: disordered and nematic phases. For details see text. From ref. 30.

The lattice distortion prior to the onset of magnetic ordering in LaFeAsO suggests the driving force may be some sort of structural instability that lifts electronic degeneracy in the sense of a Jahn–Teller or Peierls distortion. Such behaviour is indeed known from materials with highly correlated electrons with relation to superconductivity,[66–68] and currently discussed in terms of orbital ordering.[69] On this account, lifting of the d_{xz}/d_{yz}-degeneracy by Coulomb repulsion leads to uneven occupation of these orbitals that make the orthorhombic structure energetically more favourable. On the other hand, DFT calculations could not yet reproduce an orthorhombic structure of LaOFeAs without magnetic order that is more stable than the tetragonal one.

Another very interesting approach takes magnetic interactions as starting point. Spin fluctuations can lead to nematic degrees of freedom, which may break the rotational symmetry when coupled to the lattice.[70] Fernandes et al.[30] have probed such nematic fluctuations in $BaFe_2As_2$ and $BaFe_{1.84}Co_{0.16}As_2$ by measuring the C_{66} component of the elastic tensor (shear modulus) using resonant ultrasonic spectroscopy (RUS). Assuming two antiferromagnetic sublattices as shown in Fig. 11, the nematic order parameter is defined as the dot product of two sublattice magnetisations $\varphi = m_1 \cdot m_2$. In the disordered phase, the spins in the two sublattices fluctuate around the magnetization directions. In the nematic phase, the two Néel vectors are locked either parallel ($\varphi > 0$) or antiparallel ($\varphi < 0$) to each other, thus making bonds between neighbouring parallel spins contract and *vice versa*.

Effects of doping on the crystal structures

Superconductivity in $BaFe_2As_2$ was first induced by potassium-doping, which introduced holes in the FeAs-layer.[71] As shown in Fig. 12, the structural and magnetic phase transition at 140 K becomes suppressed by hole doping in a similar way to LaOFeAs by electron-doping *via* fluoride substitution ($LaO_{1−x}F_xFeAs$). Up to now, the critical temperature of 38 K is still the highest in hole-doped 122-type iron arsenide materials. The complete phase diagram of $Ba_{1−x}K_xFe_2As_2$ was readily published[72] and shows a wide superconducting dome ranging from $x = 0.15$ up to $x = 1$ as shown in Fig. 13.

While hole-doping of LaOFeAs has been realized early in $La_{1−x}Sr_xOFeAs$ ($T_c = 25$ K),[73] corresponding 'indirectly' electron-doped 122-compounds like $Sr_{1−x}La_xFe_2As_2$ ($T_c = 22$ K) have been synthesized only recently by high pressure methods.[74] An important extension was the finding that 'direct' electron-
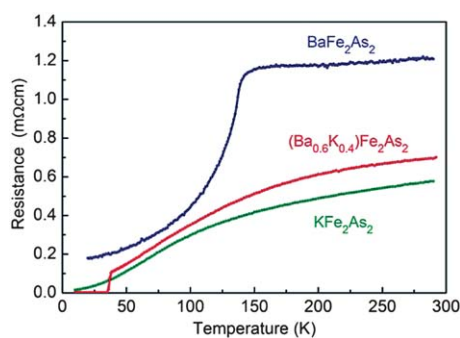

Fig. 10 Orthorhombicity of a $BeFe_2As_2$ single crystal.[61]

Fig. 12 Resistivities of $BaFe_2As_2$, KFe_2As_2 and $Ba_{0.6}K_{0.4}Fe_2As_2$.[71]

Fig. 14 Changes of structural parameters in $Ba_{1-x}K_xFe_2As_2$.[72]

doping of $BaFe_2As_2$ is also possible by substitution of cobalt for iron.[75] The phase diagram of $BaFe_{2-x}Co_xAs_2$ turned out to be similar to that of potassium-doping, only the superconducting dome is narrower and the highest T_c is about 25 K. This is very different from the cooper-oxide superconductors, where any substitution of the Cu atoms rapidly destroys superconductivity.

The structural changes that may take place by doping have not yet been studied conclusively. Fig. 14 shows how the structural parameters vary almost linearly within the solid solution of KFe_2As_2 and $BaFe_2As_2$. The unit cell volume is almost constant in spite of the slightly bigger ion radius of K^+ (1.51 Å) in comparison with Ba^{2+} (1.42 Å).[42] Due to the shrinking lattice parameter a, the Fe–Fe bond length is mostly affected and changes significantly from 2.8 to 2.72 Å. While the lengths of the strong Fe–As bonds remain constant (2.4 Å), the As–Fe–As bond angle shifts linearly from 111.1° in $BaFe_2As_2$ to 106.5° in KFe_2As_2. The highest T_c of 38 K coincides with the ideal tetra-hedral angle of 109.47°. Lee *et al.*[76] collected bond angles of many iron based superconductors and confirmed this remarkable congruence. But in spite of the apparent relation to T_c, the true role of the bond angle is still unclear. The decrease from 111.1° in $BaFe_2As_2$ to 109.5° and lower by hole-doping cannot be well understood from atom sizes alone, because substitution of other alkaline metals for barium always decreases the As–Fe–As angle. Even if barium is replaced by much smaller sodium atoms (r_{Na+} = 1.16 Å) in $Ba_{1-x}Na_xFe_2As_2$,[77] the c-axis likewise increases and the angle becomes smaller until it reaches 109.5° at $x \approx$ 0.4, where again the T_c is the highest. This suggests that the angle may also be controlled by the electron count.

An earlier publication has shown relationships between the electron count and the bonds between the metal atoms within the
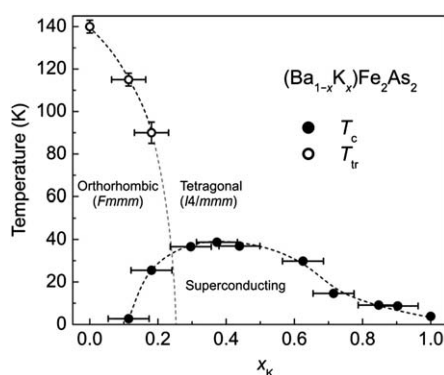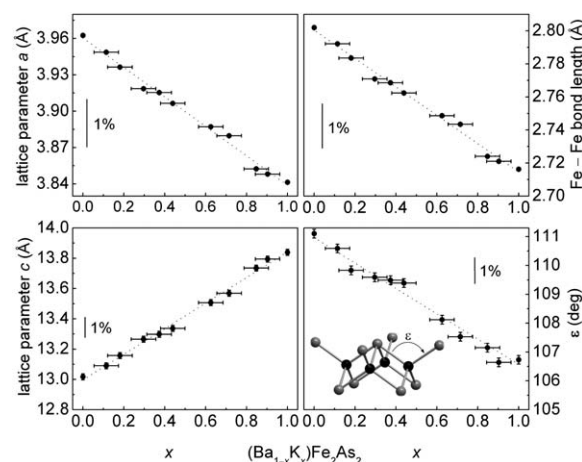
tetrahedral layer of compounds with $ThCr_2Si_2$-type structure.[78] Weak Fe–Fe $\pi\pi^*$-type antibonding bands are also close to the Fermi energy in $BaFe_2As_2$. Their depopulation by the decreased electron count of KFe_2As_2 sounds straightforward in order to explain the shorter a-axis (Fe–Fe bond lengths) and the constant volume despite the larger K-atoms and in fact shrinking also by Na-doping. However, this seemingly natural effect could not yet be proved by quantum chemical calculations.

A detailed study of the crystal structure changes by cobalt-doping has been published only recently.[79] Selected results are compiled in Fig. 15. The lattice parameters show the opposite changes than by potassium (hole) doping and the changes are even smaller. Also the allegedly important bond angle increases by Co-doping and can therefore not adopt 109.47°. In contrast to potassium-doping, the Fe–As bond length slightly increases by Co-doping and also under pressure. This quite different struc-tural behaviour of hole- and electron-doped $BaFe_2As_2$ together with the nevertheless similar phase diagrams and super-conducting domes strongly suggest that small structural changes are not the crucial factors that induce superconductivity in $BaFe_2As_2$. It seems much more probable that the charge modi-fication triggers the suppression of the magnetic order and the emergence of superconductivity.

This conclusion is convincingly supported by a most recent study of the solid solution $Ba_{1-x}K_xFe_{1.86}Co_{0.14}As_2$,[80] where the electron-doping by cobalt is compensated by hole doping with potassium at $x \approx$ 0.14. Indeed, the magnetically ordered orthorhombic phase is recovered, while supercon-ductivity emerges at lower as well as at higher potassium-concentrations.
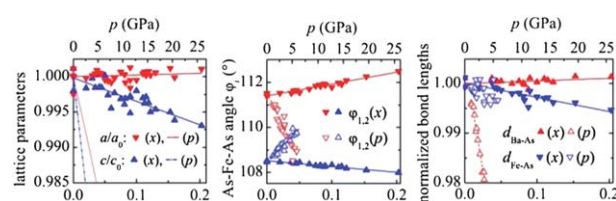

Fig. 13 Phase diagram of potassium-doped $BaFe_2As_2$.[72]

Fig. 15 Changes of structural parameters of $Ba(Fe_{1-x}Co_x)_2As_2$ by Co-concentration and pressure.[79]
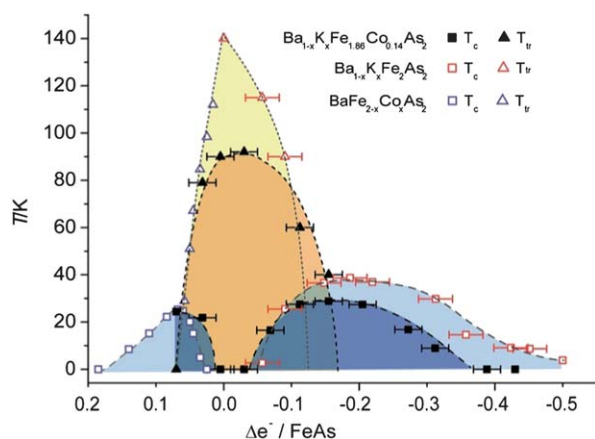
Fig. 16 Phase diagrams of potassium-, cobalt-, and K/Co combined doped $BaFe_2As_2$, showing T_c, T_S (T_{tr} in the plot) against the amount of transferred electrons per FeAs by doping.[80]

Fig. 17 c-Axis lattice parameters of $Ca_{1-x}RE_xFe_2As_2$. From Ref. 86

Fig. 16 shows the phase diagrams of potassium-, cobalt-, and K/Co combined doped $BaFe_2As_2$. Superconductivity in electron-doped $BaFe_{1.86}Co_{0.14}As_2$ ($T_c \approx 25$ K) is rapidly suppressed when the excess electrons become compensated by holes from K-doping. As soon as the charge compensated area around $\Delta e^- \approx 0$ is traversed and hole-doping outcomes, superconductivity returns and reaches a maximum T_c of ~30 K when 0.2 holes per FeAs are introduced. The lower T_c in comparison to the cobalt-free $Ba_{1-x}K_xFe_2As_2$ at $x = 0.4$ (0.2 holes per FeAs likewise) is assigned to the disorder in the FeAs-layer by cobalt-substitution.

These findings emphasize the crucial role of the charge for inducing superconductivity in iron arsenide parent compounds. I believe that the often discussed structural changes in terms of bond angles or lengths do not inherently initiate superconductivity, but are rather important to achieve the highest critical temperatures.

$CaFe_2As_2$ represents a special case among the 122-compounds. Due to the small ionic radius of Ca^{2+} one may expect the $ThCr_2Si_2$-structure to become less stable and indeed, this compound has not been described before 2008.[81] The smaller size of the calcium atoms leads to a significantly shorter c-axis (11.76 Å) and the distance between the arsenic atoms of adjacent layers approaches the range of bonding interactions. Consequently, a pressure-induced phase transition to a structure with As–As bonds has been found quickly.[82] The latter is accompanied by drastic reductions of the c-axis by 1 Å and the cell volume by nearly 5%. This phase has been referred to as "collapsed tetragonal". However, it should be mentioned that such phase transitions have been reported earlier in several other $ThCr_2Si_2$-type compounds.[83,84] $CaFe_2As_2$ becomes superconducting by hole-doping *e.g.* with sodium ($T_c \approx 26$ K).[85] More interesting is the recent report about superconductivity in rare-earth substituted, *i.e.* electron-doped $Ca_{1-x}RE_xFe_2As_2$ (RE = La–Nd) up to 45 K,[86] which is the highest critical temperature in 122-compounds so far. Surprisingly, superconductivity emerges in the "collapsed" phase which evolved by the RE substitution. It is really remarkable that the highest T_c occurs just below the structural transition temperatures, where the c-axis shrinks abruptly, as depicted in Fig. 17. This may indicate some new relation between the
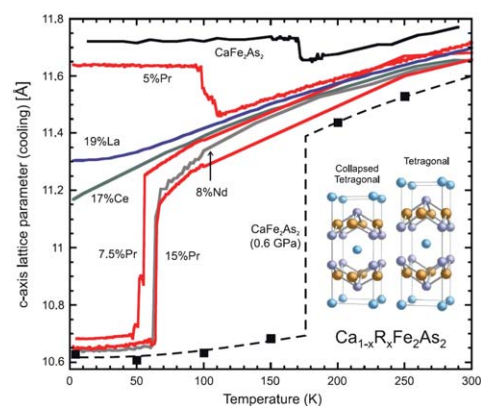
structural instability and superconductivity, even though the details remain to be seen.

Co-existence of superconductivity and magnetism

Almost all phase diagrams of iron arsenide superconductors indicate that the magnetic ordering is not abruptly and completely suppressed before superconductivity emerges. More or less pronounced overlaps in the underdoped ranges (see Fig. 7,13 and 16) suggest that either phase separation takes place or superconductivity can indeed co-exist with magnetic order. Co-existence was first proposed by Chen *et al.* for $Ba_{1-x}K_xFe_2As_2$.[87] Actually, elastic neutron scattering alone cannot distinguish between reduction of the ordered moment or a decrease in the magnetic fraction of the sample, *i.e.* phase separation. But ^{57}Fe-Mössbauer measurements as a local probe to magnetism also revealed the co-existence of magnetic ordering and superconductivity in underdoped $Ba_{1-x}K_xFe_2As_2$.[88] Fig. 18 shows the 4 K spectra of $BaFe_2As_2$ and superconducting $Ba_{0.8}K_{0.2}Fe_2As_2$ powder samples. Both are subject to very similar magnetic hyperfine field splitting that proves static magnetic ordering. No paramagnetic iron was detected in the superconducting phase, strongly suggesting homogeneous co-existence of both order parameters on an atomic length scale.

At that time, the homogeneity of $Ba_{1-x}K_xFe_2As_2$ was under debate. Especially studies on single crystals suggested phase separation into superconducting non-magnetic and magnetic non-superconducting fractions. A combined X-ray powder diffraction, neutron scattering, μSR and magnetic force microscopy study by Park *et al.*[89] suggested phase separation on a lateral scale of several tens of nanometres in single crystals grown from a tin flux. However, growing large homogeneous single crystals of $Ba_{1-x}K_xFe_2As_2$ is still very difficult, and especially the tin flux as used here is known to be problematic.[52] Nevertheless, the authors stated that this phase separation should be intrinsic to $Ba_{1-x}K_xFe_2As_2$, which is an unsupportable generalizing claim. The observed inhomogeneity may concern the used crystals, but not the material itself.

Convincing experiments about the coexistence of superconducting and magnetic order parameters were performed on cobalt-doped $BaFe_{2-x}Co_xAs_2$, where homogeneous crystals are easier to prepare. Christianson *et al.*[90] reported magnetic

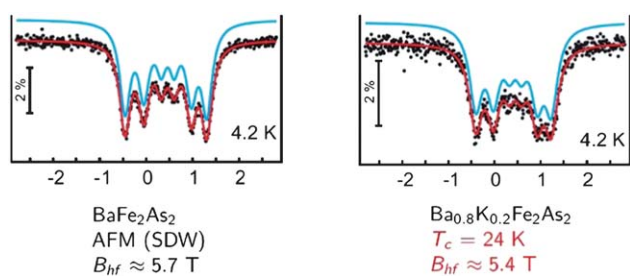**Fig. 18** ^{57}Fe-Mössbauer spectra of BaFe$_2$As$_2$ and superconducting Ba$_{0.8}$K$_{0.2}$Fe$_2$As$_2$.[88]
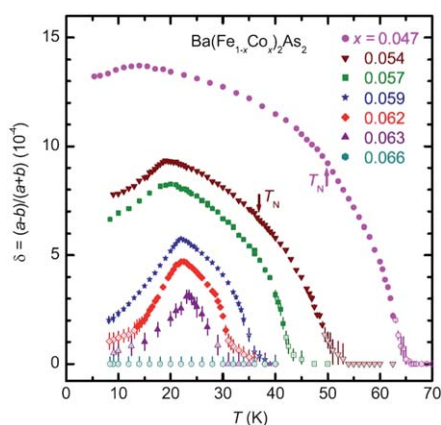
Fig. 19 Orthorhombic distortion δ of Ba(Fe$_{1-x}$Co$_x$)$_2$As$_2$ as function of temperature.[91]

scattering in superconducting BaFe$_{1.92}$Co$_{0.08}$As$_2$ and moreover, a 6% reduction of the Bragg intensity at T_c. Simultaneous inelastic scattering experiments revealed additional intensity at 4.5 meV consistent with a spin resonance emerging at T_c as found in other FeAs superconductors. This compensation of spectral weight loss in the Bragg intensity by an upcoming spin resonance at T_c provides remarkable evidence of the competition between magnetic order and superconductivity in Co-doped BaFe$_2$As$_2$.

Since the magnetic ordering is strongly coupled to the structure by the orthorhombic lattice distortion, also the orthorhombicity parameter $\delta = (a - b)/(a + b)$ can be used to detect this effect. This has impressively been shown by Nandi et al.,[91] who measured the temperature dependency of the lattice parameters extremely precisely. Fig. 19 shows the suppression of the orthorhombicity at T_c for different Co-concentrations in Ba(Fe$_{1-x}$Co$_x$)$_2$As$_2$. The effect increases as the doping level approaches the optimal value of ~0.07, where the distortion vanishes and the material is tetragonal. Close to this value, the orthorhombicity gets almost completely suppressed at temperatures $T < T_c$ (see $x = 0.063$). Nevertheless the compound remains orthorhombic and the term 're-entrant tetragonal phase' is therefore somewhat misleading. Note that these data are based on measurements of one single Bragg peak (1110) only, while the detailed crystal structures of the low temperature phases were not yet determined. Recently, the reduction of the orthorhombicity at T_c was also shown for the hole-doped system Ba$_{1-x}$K$_x$Fe$_2$As$_2$.[92]

Concluding remarks

This feature article is a brief overview in order to give a flavour of this lively field from the view of the solid state chemist. The diversity of physical properties of these seemingly chemically simple compounds is amazing and the progress within the last 3 years is impressive. Nevertheless, we should remember that the cornerstones to these materials were laid in the 1980s by solid state chemists who discovered all these compounds and determined their structures. This teaches us the lesson that explorative synthesis continuous to be indispensable in order to discover new superconductors.

The field of iron based superconductors grows rapidly; therefore it is hardly possible to conclusively summarize the current state. In my opinion, iron based materials have significantly consolidated the connection between magnetism and superconductivity, even though a final theory of pairing mediated by spin fluctuations is still missing. Since the magnetism is uniquely coupled to structural order parameters, the experience and intuition of the solid state chemist is especially demanded. The sustainability of the Fermi surface nesting concept remains to be seen. Seemingly it works well to rationalize the structural and magnetic instabilities (with the exception of LiFeAs), even though their underlying origin is still not completely understood. But it is less clear than ever whether nesting is truly essential to superconductivity or to the proposed $s^{\pm}$ gap symmetry. The November 2010 discovery of iron selenide superconductors like K$_x$Fe$_{2-y}$Se$_2$ ($T_c \approx 30$ K)[22] with ThCr$_2$Si$_2$-type structure and a manifold of new magnetic properties[93] casts significant doubts on this concept,[94] because these new materials lack just those features that were considered essential. Nevertheless, this next class of iron-based materials holds a lot of new opportunities for structural chemistry, because a special kind of temperature-dependent iron vacancy ordering[95] plays an important role. It is delightful to see how this field produces the next surprise and again captivates material scientists with new questions. Superconductivity research is lively and more attractive than ever at 100.

Acknowledgements

Notes and references

1 W. E. Pickett, Physica. B (Amsterdam), 2001, **296**, 112.
2 Y. Kamihara, H. Hiramatsu, M. Hirano, R. Kawamura, H. Yanagi, T. Kamiya and H. Hosono, J. Am. Chem. Soc., 2006, **128**, 10012.
3 Y. Kamihara, T. Watanabe, M. Hirano and H. Hosono, J. Am. Chem. Soc., 2008, **130**, 3296.
4 Z.-A. Ren, W. Lu, J. Yang, W. Yi, X.-L. Shen, Z.-C. Li, G.-C. Che, X.-L. Dong, L.-L. Sun, F. Zhou and Z.-X. Zhao, Chin. Phys. Lett., 2008, **25**, 2215.
5 I. I. Mazin, Nature, 2010, **464**, 183.
6 D. C. Johnston, Adv. Phys., 2010, **59**, 803.
7 P. Monthoux, A. V. Balatsky and D. Pines, Phys. Rev. B: Condens. Matter, 1992, **46**, 14803.
8 J. R. Kirtley, C. C. Tsuei, J. Z. Sun, C. C. Chi, L. S. Yu-Jahnes, A. Gupta, M. Rupp and M. B. Ketchen, Nature, 1995, **373**, 225.
9 I. I. Mazin, D. J. Singh, M. D. Johannes and M. H. Du, Phys. Rev. Lett., 2008, **101**, 057003.

10 T. Katase, H. Hiramatsu, H. Yanagi, T. Kamiya, M. Hirano and H. Hosono, *Solid State Commun.*, 2009, **149**, 2121.

11 M. Kidszun, S. Haindl, T. Thersleff, J. Werner, M. Langer, J. Hanisch, K. Iida, E. Reich, L. Schultz and B. Holzapfel, *Europhys. Lett.*, 2010, **90**, 57005.

12 Y. Mizuguchi, K. Deguchi, S. Tsuda, T. Yamaguchi, H. Takeya, H. Kumakura and Y. Takano, *Appl. Phys. Express*, 2009, **2**, 083004.

13 P. M. Shirage, K. Miyazawa, K. Kihou, H. Kito, Y. Yoshida, Y. Tanaka, H. Eisaki and A. Iyo, *Phys. Rev. Lett.*, 2010, **105**, 037004.

14 R. H. Liu, T. Wu, G. Wu, H. Chen, X. F. Wang, Y. L. Xie, J. J. Ying, Y. J. Yan, Q. J. Li, B. C. Shi, W. S. Chu, Z. Y. Wu and X. H. Chen, *Nature*, 2009, **459**, 64.

15 P. M. Shirage, K. Kihou, K. Miyazawa, C. H. Lee, H. Kito, H. Eisaki, T. Yanagisawa, Y. Tanaka and A. Iyo, *Phys. Rev. Lett.*, 2009, **103**, 0257003.

16 G. Hägg and A. L. Kindström, *Z. Phys. Chem. B*, 1933, **22**, 453.

17 R. Juza and K. Langer, *Z. Anorg. Allg. Chem.*, 1968, **361**, 58.

18 D. R. Parker, M. J. Pitcher, P. J. Baker, I. Franke, T. Lancaster, S. J. Blundell and S. J. Clarke, *Chem. Commun.*, 2009, **16**, 2189.

19 V. Johnson and W. Jeitschko, *J. Solid State Chem.*, 1974, **11**, 161.

20 P. Quebe, L. J. Terbüchte and W. Jeitschko, *J. Alloys Compd.*, 2000, **302**, 70.

21 P. Pfisterer and G. Nagorsen, *Z. Naturforsch., B: Anorg. Chem., Org. Chem*, 1980, **35**, 703.

22 J. Guo, S. Jin, G. Wang, S. Wang, K. Zhu, T. Zhou, M. He and X. Chen, *Phys. Rev. B: Condens. Matter Mater. Phys.*, 2010, **82**, 180520.

23 X. Zhu, F. Han, G. Mu, P. Cheng, B. Shen, B. Zeng and H.-H. Wen, *Phys. Rev. B: Condens. Matter Mater. Phys.*, 2009, **79**, 220512.

24 W. J. Zhu and P. H. Hor, *Inorg. Chem.*, 1997, **36**, 3576.

25 J. Dong, H. J. Zhang, G. Xu, Z. Li, G. Li, W. Z. Hu, D. Wu, G. F. Chen, X. Dai, J. L. Luo, Z. Fang and N. L. Wang, *Europhys. Lett.*, 2008, **83**, 27006.

26 S. Lebegue, *Phys. Rev. B: Condens. Matter Mater. Phys.*, 2007, **75**, 035110.

27 F. Ma and Z.-Y. Lu, *Phys. Rev. B: Condens. Matter Mater. Phys.*, 2008, **78**, 033111.

28 D. J. Singh and M. H. Du, *Phys. Rev. Lett.*, 2008, **100**, 237003.

29 R. A. Borzi, S. A. Grigera, J. Farrell, R. S. Perry, S. J. S. Lister, S. L. Lee, D. A. Tennant, Y. Maeno and A. P. Mackenzie, *Science*, 2007, **315**, 214.

30 R. M. Fernandes, L. H. VanBebber, S. Bhattacharya, P. Chandra, V. Keppens, D. Mandrus, M. A. McGuire, B. C. Sales, A. S. Sefat and J. Schmalian, *Phys. Rev. Lett.*, 2010, **105**, 157003.

31 C. de la Cruz, Q. Huang, J. W. Lynn, J. Y. Li, W. Ratcliff, J. L. Zarestky, H. A. Mook, G. F. Chen, J. L. Luo, N. L. Wang and P. C. Dai, *Nature*, 2008, **453**, 899.

32 T. Nomura, S. W. Kim, Y. Kamihara, M. Hirano, P. V. Sushko, K. Kato, M. Takata, A. L. Shluger and H. Hosono, *Supercond. Sci. Technol.*, 2008, **21**, 125028.

33 N. Qureshi, Y. Drees, J. Werner, S. Wurmehl, C. Hess, R. Klingeler, B. Büchner, M. T. Fernandez-Diaz and M. Braden, *Phys. Rev. B: Condens. Matter Mater. Phys.*, 2010, **82**, 184521.

34 H. F. Li, W. Tian, J. Q. Yan, J. L. Zarestky, R. W. McCallum, T. A. Lograsso and D. Vaknin, *Phys. Rev. B: Condens. Matter Mater. Phys.*, 2010, **82**, 064409.

35 H. Luetkens, H. H. Klauss, M. Kraken, F. J. Litterst, T. Dellmann, R. Klingeler, C. Hess, R. Khasanov, A. Amato, C. Baines, M. Kosmala, O. J. Schumann, M. Braden, J. Hamann-Borrero, N. Leps, A. Kondrat, G. Behr, J. Werner and B. Buchner, *Nat. Mater.*, 2009, **8**, 305.

36 M. J. Pitcher, D. R. Parker, P. Adamson, S. J. C. Herkelrath, A. T. Boothroyd, R. M. Ibberson, M. Brunelli and S. J. Clarke, *Chem. Commun.*, 2008, 5918.

37 X. C. Wang, Q. Q. Liu, Y. X. Lv, W. B. Gao, L. X. Yang, R. C. Yu, F. Y. Li and C. Q. Jin, *Solid State Commun.*, 2008, **148**, 538.

38 J. H. Tapp, Z. J. Tang, B. Lv, K. Sasmal, B. Lorenz, P. C. W. Chu and A. M. Guloy, *Phys. Rev. B: Condens. Matter Mater. Phys.*, 2008, **78**, 060505.

39 S. V. Borisenko, V. B. Zabolotnyy, D. V. Evtushinsky, T. K. Kim, I. V. Morozov, A. N. Yaresko, A. A. Kordyuk, G. Behr, A. Vasiliev, R. Follath and B. Büchner, *Phys. Rev. Lett.*, 2010, **105**, 067002.

40 D. J. Singh, *Phys. Rev. B: Condens. Matter Mater. Phys.*, 2008, **78**, 094511.

41 Y. F. Li and B. G. Liu, *Eur. Phys. J. B*, 2009, **72**, 153.

42 R. D. Shannon and C. T. Prewitt, *Acta Crystallogr., Sect. B: Struct. Crystallogr. Cryst. Chem.*, 1969, **25**, 925.

43 M. J. Pitcher, T. Lancaster, J. D. Wright, I. Franke, A. J. Steele, P. J. Baker, F. L. Pratt, W. T. Thomas, D. R. Parker, S. J. Blundell and S. J. Clarke, *J. Am. Chem. Soc.*, 2010, **132**, 10467.

44 K. Sasmal, B. Lv, Z. J. Tang, F. Chen, Y. Y. Xue, B. Lorenz, A. M. Guloy and C. W. Chu, *Phys. Rev. B: Condens. Matter Mater. Phys.*, 2009, **79**, 184516.

45 S. Li, C. de la Cruz, Q. Huang, G. F. Chen, T. L. Xia, J. L. Luo, N. L. Wang and P. Dai, *Phys. Rev. B: Condens. Matter Mater. Phys.*, 2009, **80**, 020504.

46 G. F. Chen, W. Z. Hu, J. L. Luo and N. L. Wang, *Phys. Rev. Lett.*, 2009, **102**, 227004.

47 C. He, Y. Zhang, B. P. Xie, X. F. Wang, L. X. Yang, B. Zhou, F. Chen, M. Arita, K. Shimada, H. Namatame, M. Taniguchi, X. H. Chen, J. P. Hu and D. L. Feng, *Phys. Rev. Lett.*, 2010, **105**, 117002.

48 D. R. Parker, M. J. P. Smith, T. Lancaster, A. J. Steele, I. Franke, P. J. Baker, F. L. Pratt, M. J. Pitcher, S. J. Blundell and S. J. Clarke, *Phys. Rev. Lett.*, 2010, **104**, 057007.

49 I. Todorov, D. Y. Chung, H. Claus, C. D. Malliakas, A. P. Douvalis, T. Bakas, J. He, V. P. Dravid and M. G. Kanatzidis, *Chem. Mater.*, 2010, **22**, 3916.

50 M. Gooch, B. Lv, K. Sasmal, J. H. Tapp, Z. J. Tang, A. M. Guloy, B. Lorenz and C. W. Chu, *Phys. C (Amsterdam, Neth.)*, 2010, **470**, S276.

51 M. Rotter, M. Tegel, I. Schellenberg, W. Hermes, R. Pöttgen and D. Johrendt, *Phys. Rev. B: Condens. Matter Mater. Phys.*, 2008, **78**, 020503(R).

52 Y. Su, P. Link, A. Schneidewind, T. Wolf, P. Adelmann, Y. Xiao, M. Meven, R. Mittal, M. Rotter, D. Johrendt, T. Brückel and M. Loewenhaupt, *Phys. Rev. B: Condens. Matter Mater. Phys.*, 2009, **79**, 064504.

53 Q. Huang, Y. Qiu, W. Bao, M. A. Green, J. W. Lynn, Y. C. Gasparovic, T. Wu, G. Wu and X. H. Chen, *Phys. Rev. Lett.*, 2008, **101**, 257003.

54 M. Kofu, Y. Qiu, W. Bao, S. H. Lee, S. Chang, T. Wu, G. Wu and X. H. Chen, *New J. Phys.*, 2009, **11**, 055001.

55 C. Krellner, N. Caroca-Canales, A. Jesche, H. Rosner, A. Ormeci and C. Geibel, *Phys. Rev. B: Condens. Matter Mater. Phys.*, 2008, **78**.

56 M. Tegel, M. Rotter, V. Weiss, F. Schappacher, R. Pöttgen and D. Johrendt, *J. Phys.: Condens. Matter*, 2008, **20**, 452201.

57 J. Zhao, W. Ratcliff, J. W. Lynn, G. F. Chen, J. L. Luo, N. L. Wang, J. Hu and P. Dai, *Phys. Rev. B: Condens. Matter Mater. Phys.*, 2008, **78**, 140504.

58 L. W. Harriger, A. Schneidewind, S. Li, J. Zhao, Z. Li, W. Lu, X. Dong, F. Zhou, Z. Zhao, J. Hu and P. Dai, *Phys. Rev. Lett.*, 2009, **103**, 087005.

59 S. D. Wilson, Z. Yamani, C. R. Rotundu, B. Freelon, E. Bourret-Courchesne and R. J. Birgeneau, *Phys. Rev. B: Condens. Matter Mater. Phys.*, 2009, **79**, 184519.

60 S. D. Wilson, C. R. Rotundu, Z. Yamani, P. N. Valdivia, B. Freelon, E. Bourret-Courchesne and R. J. Birgeneau, *Phys. Rev. B: Condens. Matter Mater. Phys.*, 2010, **81**, 14501.

61 M. G. Kim, R. M. Fernandes, A. Kreyssig, J. W. Kim, A. Thaler, S. L. Bud'ko, P. C. Canfield, R. J. McQueeney, J. Schmalian and A. I. Goldman, *Phys. Rev. B: Condens. Matter Mater. Phys.*, 2011, **83**, 134522.

62 M. Tegel, S. Johansson, V. Weiß, I. Schellenberg, W. Hermes, R. Pöttgen and D. Johrendt, *Europhys. Lett.*, 2008, **84**, 67007.

63 Y. Xiao, Y. Su, R. Mittal, T. Chatterji, T. Hansen, S. Price, C. M. N. Kumar, J. Persson, S. Matsuishi, Y. Inoue, H. Hosono and T. Brueckel, *Phys. Rev. B: Condens. Matter Mater. Phys.*, 2010, **81**, 094523.

64 A. Ricci, N. Poccia, B. Joseph, L. Barba, G. Arrighetti, G. Ciasca, J. Q. Yan, R. W. McCallum, T. A. Lograsso, N. D. Zhigadlo, J. Karpinski and A. Bianconi, *Phys. Rev. B: Condens. Matter Mater. Phys.*, 2010, **82**, 144507.

65 A. Cano, M. Civelli, I. Eremin and I. Paul, *Phys. Rev. B: Condens. Matter Mater. Phys.*, 2010, **82**, 020408.

66 D. Bichler, V. Zinth, D. Johrendt, O. Heyer, M. K. Forthaus, T. Lorenz and M. M. Abd-Elmeguid, *Phys. Rev. B: Condens. Matter Mater. Phys.*, 2008, **77**, 212102.

67 R. Pocha, D. Johrendt and R. Pöttgen, *Chem. Mater.*, 2000, **12**, 2882.

This journal is © The Royal Society of Chemistry 2011

J. Mater. Chem., 2011, **21**, 13726–13736 | 13735

68 R. Pocha, D. Johrendt, B. Ni and M. M. Abd-Elmeguid, *J. Am. Chem. Soc.*, 2005, **127**, 8732.
69 W. Lv, J. Wu and P. Phillips, *Phys. Rev. B: Condens. Matter Mater. Phys.*, 2009, **80**, 224506.
70 C. Fang, H. Yao, W.-F. Tsai, J. Hu and S. A. Kivelson, *Phys. Rev. B: Condens. Matter Mater. Phys.*, 2008, **77**, 224509.
71 M. Rotter, M. Tegel and D. Johrendt, *Phys. Rev. Lett.*, 2008, **101**, 107006.
72 M. Rotter, M. Pangerl, M. Tegel and D. Johrendt, *Angew. Chem., Int. Ed.*, 2008, **47**, 7949.
73 H.-H. Wen, G. Mu, L. Fang, H. Yang and X. Zhu, *Europhys. Lett.*, 2008, **82**, 17009.
74 Y. Muraba, S. Matsuishi, S.-W. Kim, T. Atou, O. Fukunaga and H. Hosono, *Phys. Rev. B: Condens. Matter Mater. Phys.*, 2010, **82**, 180512.
75 A. S. Sefat, R. Jin, M. A. McGuire, B. C. Sales, D. J. Singh and D. Mandrus, *Phys. Rev. Lett.*, 2008, **101**, 117004.
76 C. H. Lee, A. Iyo, H. Eisaki, H. Kito, M. T. Fernandez-Diaz, T. Ito, K. Kihou, H. Matsuhata, M. Braden and K. Yamada, *J. Phys. Soc. Jpn.*, 2008, **77**, 083704.
77 R. Cortes-Gil, D. R. Parker, M. J. Pitcher, J. Hadermann and S. J. Clarke, *Chem. Mater.*, 2010, **22**, 4304.
78 D. Johrendt, C. Felser, O. Jepsen, O. K. Andersen, A. Mewis and J. Rouxel, *J. Solid State Chem.*, 1997, **130**, 254.
79 S. Drotziger, P. Schweiss, K. Grube, T. Wolf, P. Adelmann, C. Meingast and H. v. Löhneysen, *J. Phys. Soc. Jpn.*, 2010, **79**, 124705.
80 V. Zinth, T. Dellmann, H.-H. Klauss and D. Johrendt, *Angew. Chem., Int. Ed.*, 2011, DOI: 10.1002/anie.201102866.
81 F. Ronning, *et al.*, *J. Phys.: Condens. Matter*, 2008, **20**, 322201.
82 A. Kreyssig, M. A. Green, Y. Lee, G. D. Samolyuk, P. Zajdel, J. W. Lynn, S. L. Bud'ko, M. S. Torikachvili, N. Ni, S. Nandi, J. B. Leao, S. J. Poulton, D. N. Argyriou, B. N. Harmon, R. J. McQueeney, P. C. Canfield and A. I. Goldman, *Phys. Rev. B: Condens. Matter Mater. Phys.*, 2008, **78**, 184517.
83 C. Huhnt, G. Michels, M. Roepke, W. Schlabitz, A. Wurth, D. Johrendt and A. Mewis, *Physica B (Amsterdam)*, 1997, **240**, 26.
84 A. Wurth, D. Johrendt, A. Mewis, C. Huhnt, G. Michels, M. Roepke and W. Schlabitz, *Z. Anorg. Allg. Chem.*, 1997, **623**, 1418.
85 P. M. Shirage, K. Miyazawa, H. Kito, H. Eisaki and A. Iyo, *Appl. Phys. Express*, 2008, **1**, 081702.
86 S. R. Saha, N. P. Butch, T. Drye, J. Magill, S. Ziemak, K. Kirshenbaum, P. Y. Zavalij, J. W. Lynn and J. Paglione, arXiv:1105.4798, (unpublished).
87 H. Chen, Y. Ren, Y. Qiu, W. Bao, R. H. Liu, G. Wu, T. Wu, Y. L. Xie, X. F. Wang, Q. Huang and X. H. Chen, *Europhys. Lett.*, 2009, **85**, 17006.
88 M. Rotter, M. Tegel, I. Schellenberg, F. M. Schappacher, R. Pöttgen, J. Deisenhofer, A. Gunther, F. Schrettle, A. Loidl and D. Johrendt, *New J. Phys.*, 2009, **11**, 025014.
89 J. T. Park, D. S. Inosov, C. Niedermayer, G. L. Sun, D. Haug, N. B. Christensen, R. Dinnebier, A. V. Boris, A. J. Drew, L. Schulz, T. Shapoval, U. Wolff, V. Neu, X. Yang, C. T. Lin, B. Keimer and V. Hinkov, *Phys. Rev. Lett.*, 2009, **102**, 117006.
90 A. D. Christianson, M. D. Lumsden, S. E. Nagler, G. J. MacDougall, M. A. McGuire, A. S. Sefat, R. Jin, B. C. Sales and D. Mandrus, *Phys. Rev. Lett.*, 2009, **103**, 087002.
91 S. Nandi, M. G. Kim, A. Kreyssig, R. M. Fernandes, D. K. Pratt, A. Thaler, N. Ni, S. L. Budko, P. C. Canfield, J. Schmalian, R. J. McQueeney and A. I. Goldman, *Phys. Rev. Lett.*, 2010, **104**, 057006.
92 E. Wiesenmayer, F. Hummel, G. Friederichs and D. Johrendt, in *International Workshop on Novel Superconductors and Super Materials 2011*, Tokyo, March 6–8, 2011.
93 F. Ye, S. Chi, W. Bao, X. F. Wang, J. J. Ying, X. H. Chen, H. D. Wang and M. F. C. H . Dong, arXiv:1102.2882, (unpublished).
94 I. Mazin, *Physics*, 2011, **4**, 26.
95 V. Y. Pomjakushin, D. V. Sheptyakov, E. V. Pomjakushina, A. Krzton-Maziopa, K. Conder, D. Chernyshov, V. Svitlyk and Z. Shermadini, *Phys. Rev. B: Condens. Matter Mater. Phys.*, 2011, **83**, 144410.